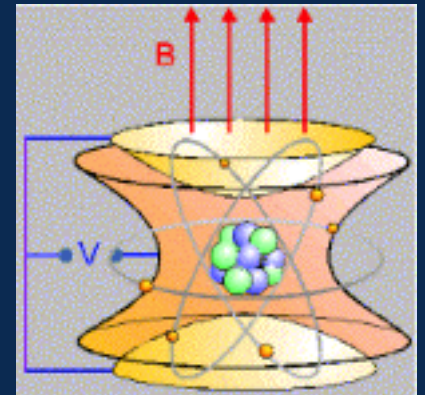


New Approaches (CoBRA, ECHO, Q-Value determination)

Valentina Lozza



ECHO Experiment



- Measure the neutrino mass
- Double Beta Decay process
- The COBRA Experiment
 - Location
 - Isotope
 - Detector working principle
 - Background/signal discrimination
- Electron Capture and Double Electron Capture process
- Q-value determination: Penning-traps (ISOLTRAP)
 - Working principle
 - Isotopes investigate
- The ECHO Experiment
 - Isotope
 - Detector Working principle
 - Detector's tests

Measure the neutrino mass

Oscillation measurements

- relative masses
- provide lower bound
 - $m_1 = 0$ (normal)
 - $m_3 = 0$ (inverted)

Direct kinematic measurements model independent

Time of flight from supernovae model dependent

$0\nu\beta\beta$ decay (model dependent)

- if neutrinos are Majorana particles
- accurate calculation of nuclear matrix element

Cosmology and astrophysics (model dependent)

- measures Σm_ν
- based on assumptions of number density in early Universe and cosmological model(s)

Δm_{ij}

m_{bb}

m_ν

Σm_i

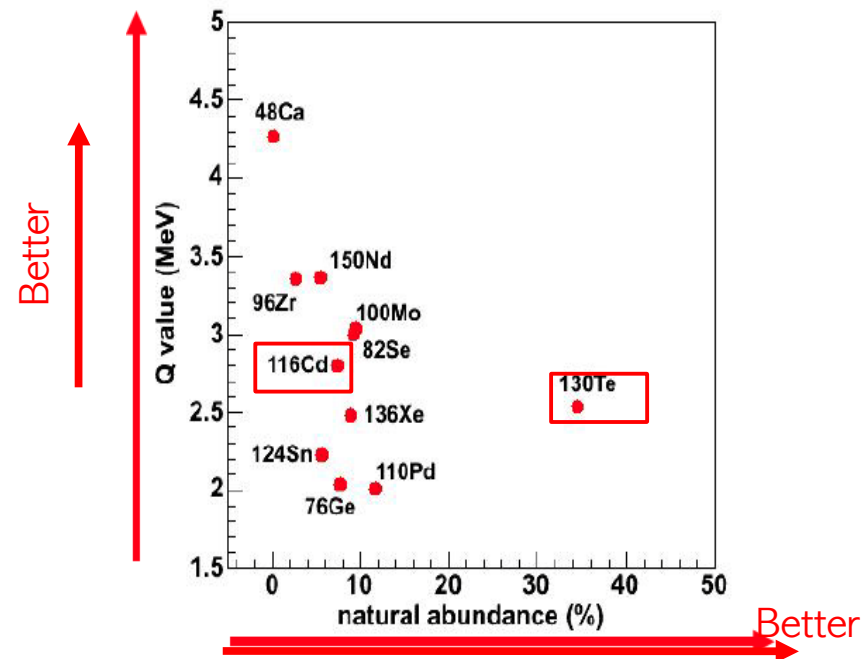
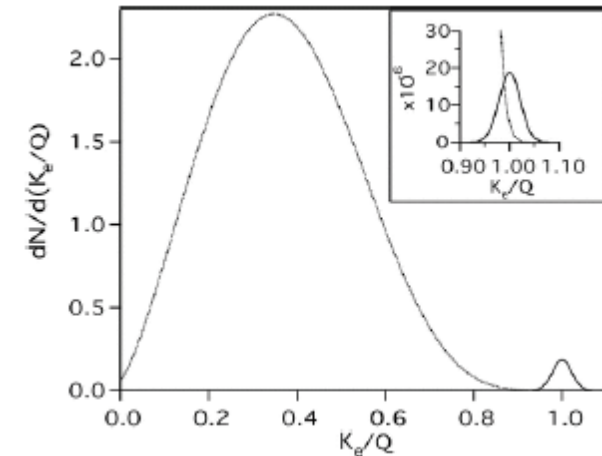


- Can only happen if neutrinos are Majorana particles
- From the events in the signal peak it is possible to determine the half-life of the decay

$$(T_{1/2}^{0\nu})^{-1} = G^{0\nu} |M^{0\nu}|^2 \left(\frac{\langle m_\nu \rangle}{m_e} \right)^2$$

$M^{0\nu}$ is model dependent → major theoretical challenge today

35 known isotopes





TU Dortmund
TU Dresden

Freiburg Materials
Research Center

University of Hamburg
University of Erlangen



Czech Technical
University in Prague



Laboratori Nazionali
del Gran Sasso



Washington University
at St. Louis



University of Bratislava



University of Jyvaskyla



University of La Plata



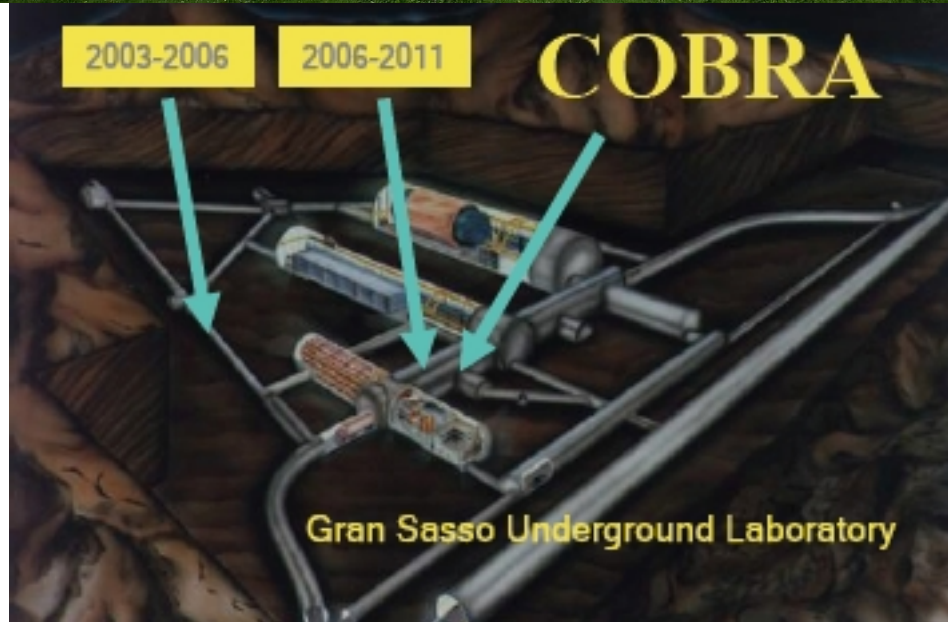
JINR Dubna

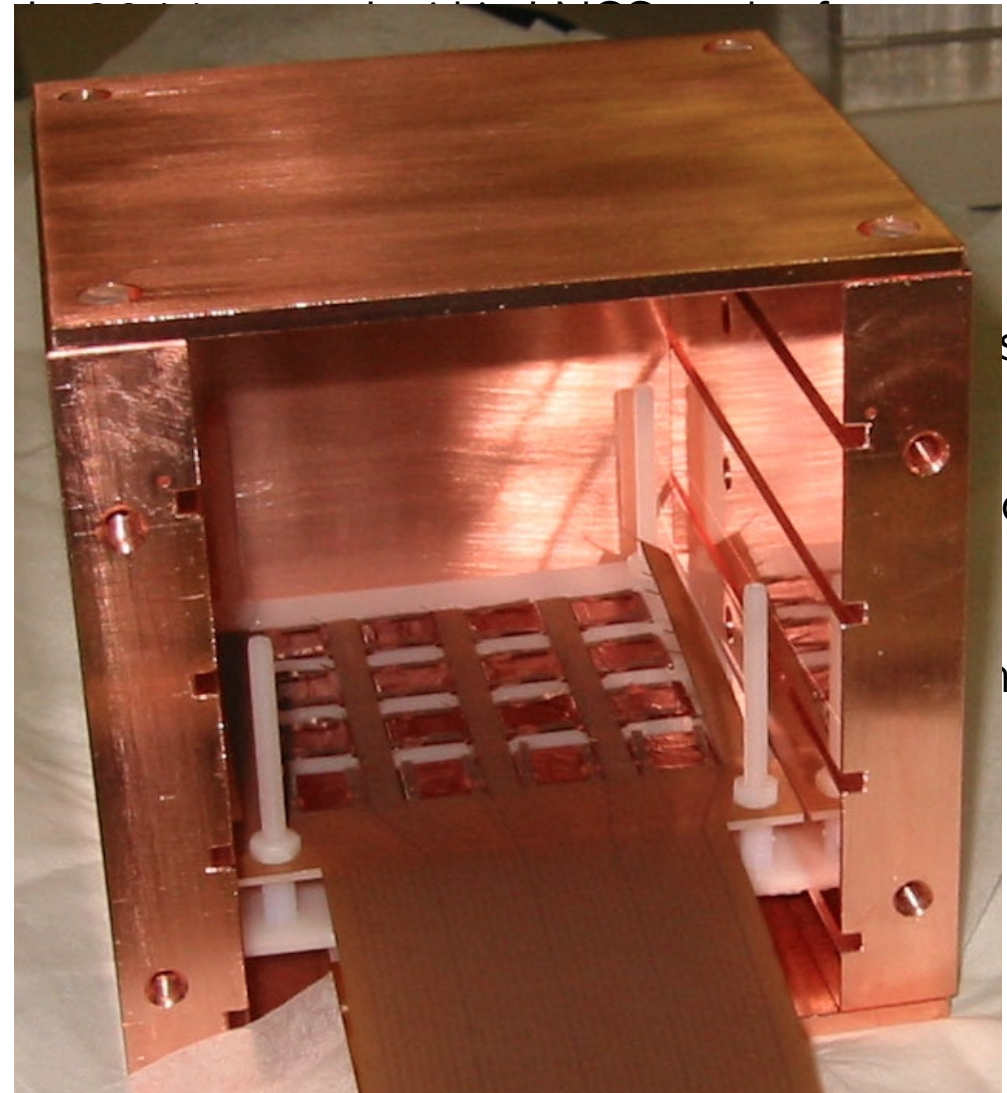
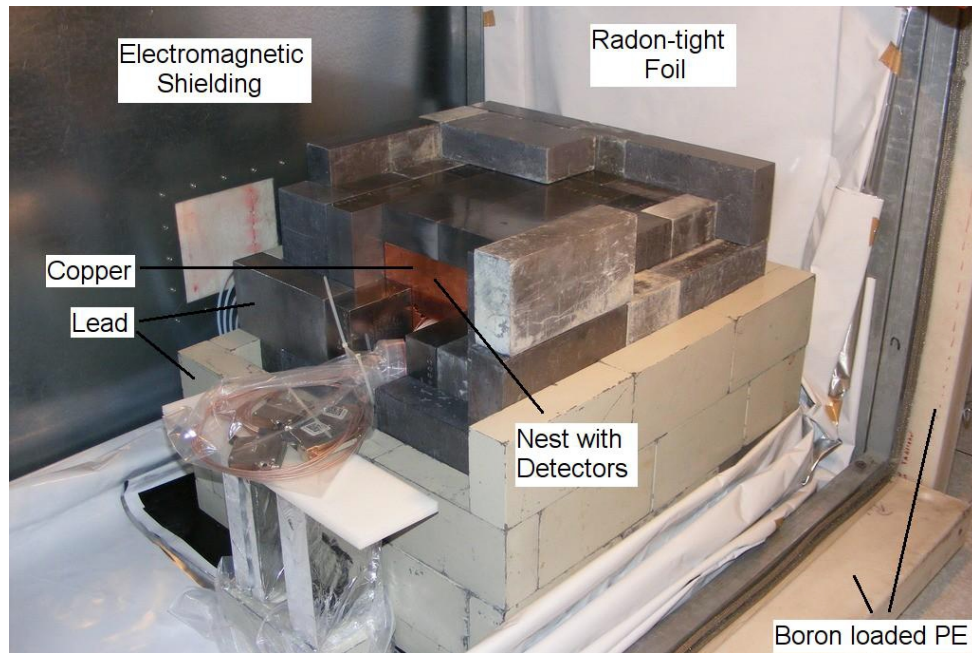
Supporting Institutes: Jagellonian University(Poland), University
of Michigan (USA)

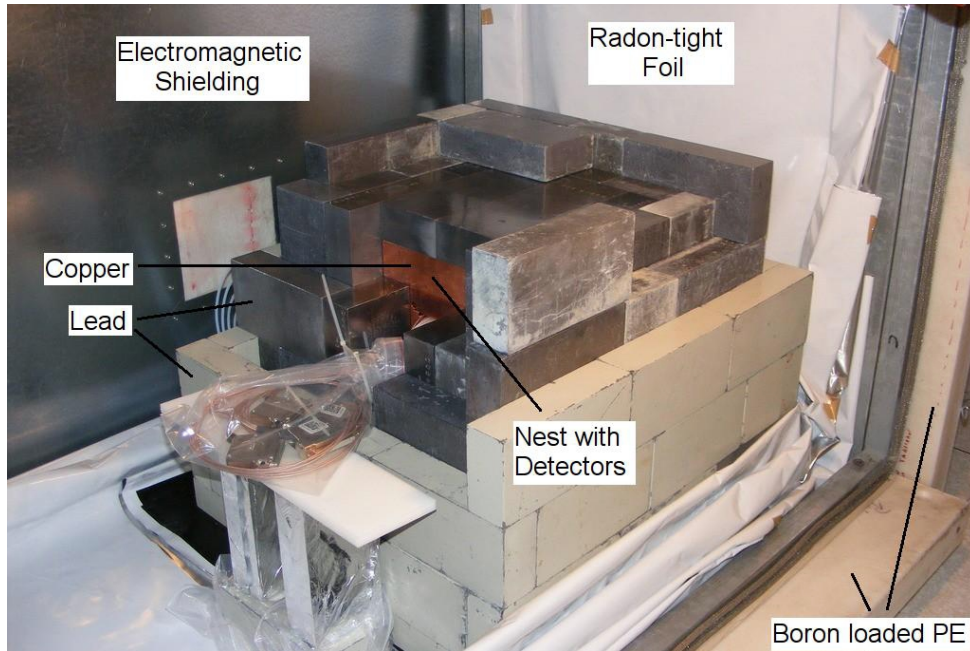
Slides from: O. Schultz, NDM2012, Nara 11-16 June 2012
C. Oldorf, TAUP2011, Munich, 5-9 September 2011
M. Frittz courtesy



COBRA experimental setup located at
Laboratori Nazionali del Gran Sasso
(LNGS), Italy
(1400 m under Gran-Sasso massif,
3700 m.w.e.)







In 2011 moved within LNGS to the former HdM Building

- Copper holder for 4 Delrin (POM) crystal layers, with 16 detectors each (for 1 cm³ CPG)
- Lead shielding with clean lead in inner layers and copper core
- Pb-shield enclosed in Rn-tight foil
- 70 mm borated PE plates as Neutron shield
- Tight Faraday-Cage (EMI shield)
- Radon shielding and N₂ flushing
- Colorless detector to reduce contamination



- New DAQ chain
- New amplifiers
- New Faraday cage
- Fully digital read-out

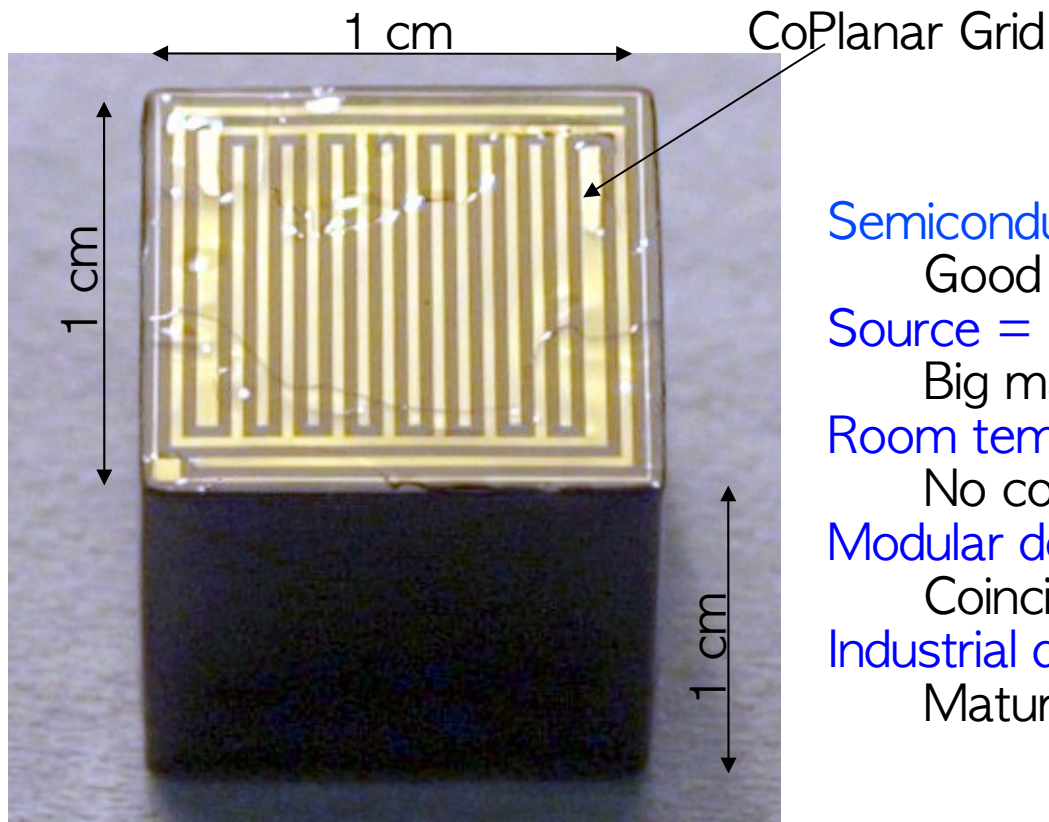


Cadmium-Zinc-Telluride 0-neutrino double-Beta Research Apparatus

Total mass of 420 kg, enriched in ^{116}Cd

Sensitivity: $T_{1/2}^{0\nu} > 10^{26} \text{ yr}$ ($m_\nu \approx 50 \text{ meV}$)

Total of 64 detectors (32 running)



Semiconductor detector

Good energy resolution, intrinsically clean material

Source = Detector

Big mass and high detection efficiency

Room temperature

No cooling needed

Modular design

Coincidence analysis

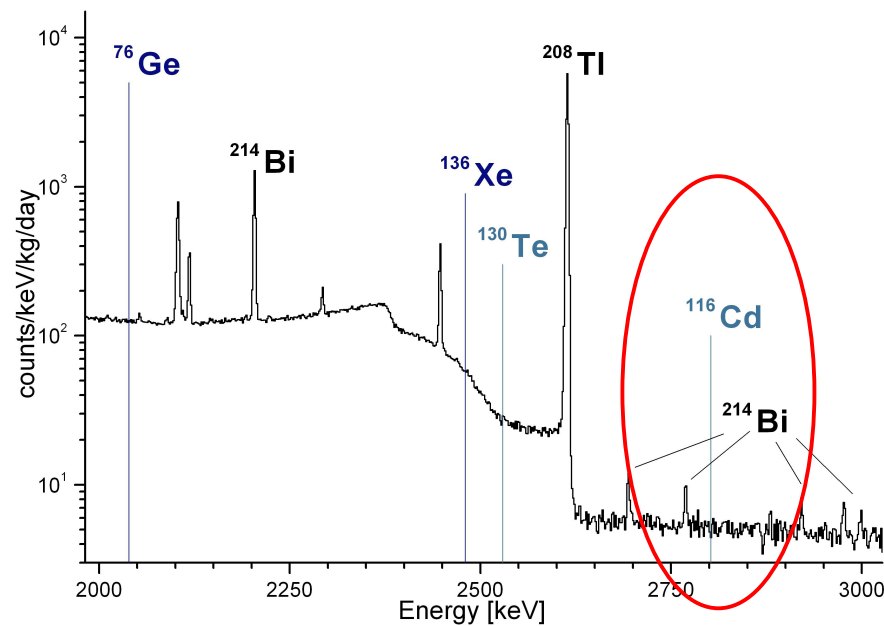
Industrial development of CdZnTe detectors

Maturing technology

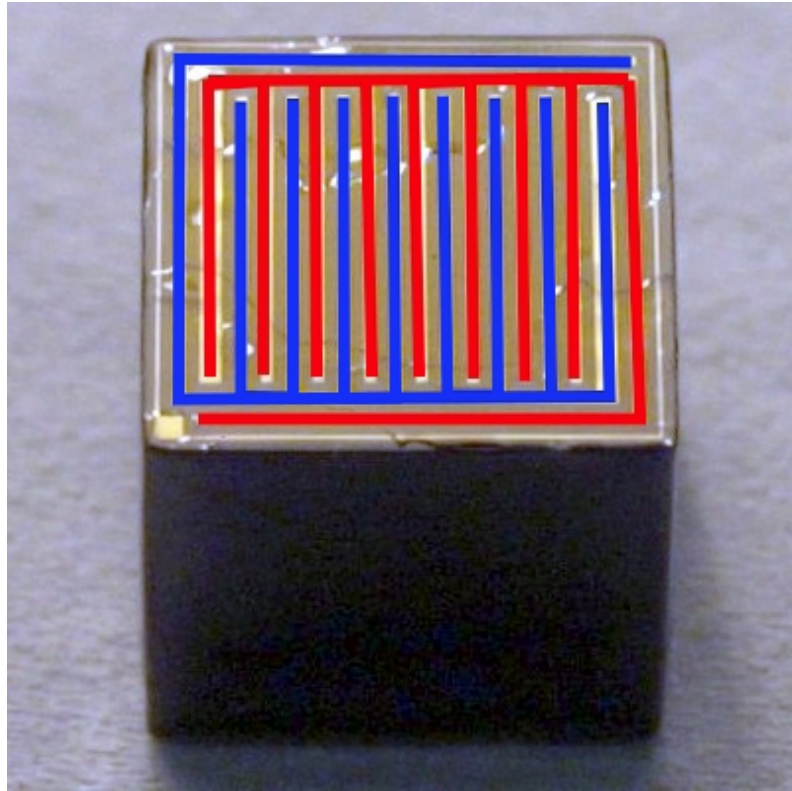


CdZnTe contains 9 0v2bcandidates, the most important:

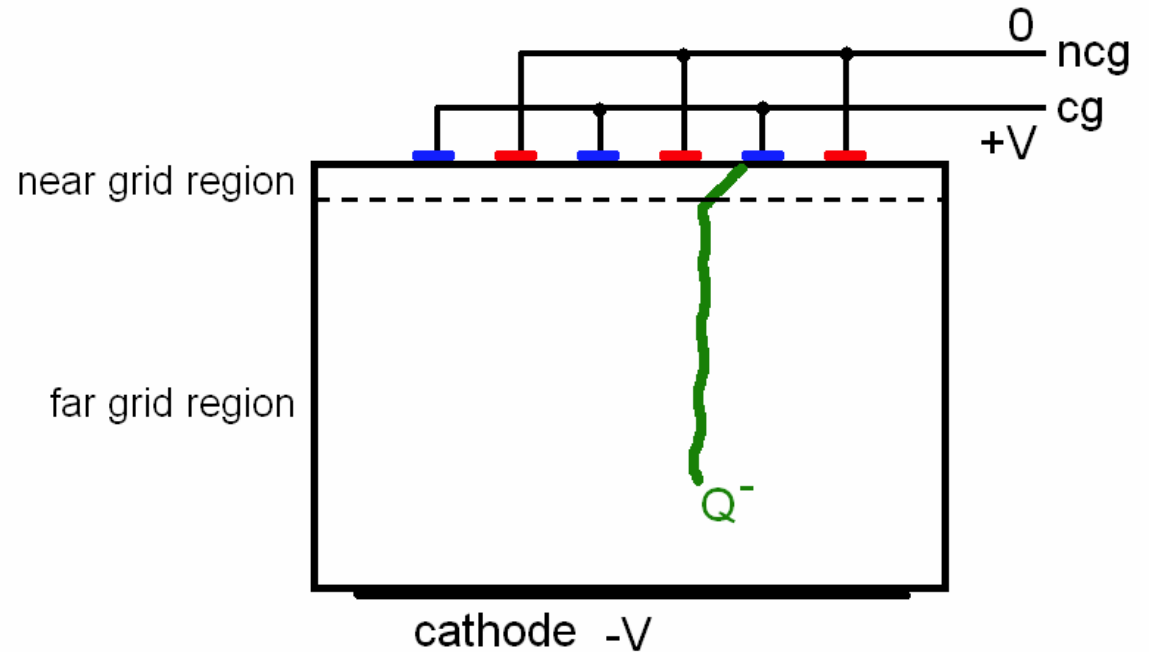
	Q [keV]	Mode	Nat. Ab [%]
^{116}Cd	2814	b^-b^-	7.5
^{106}Cd	2771	b^+b^+	1.2
^{130}Te	2527	b^-b^-	33.8



C. Oldorf, TAUP2011

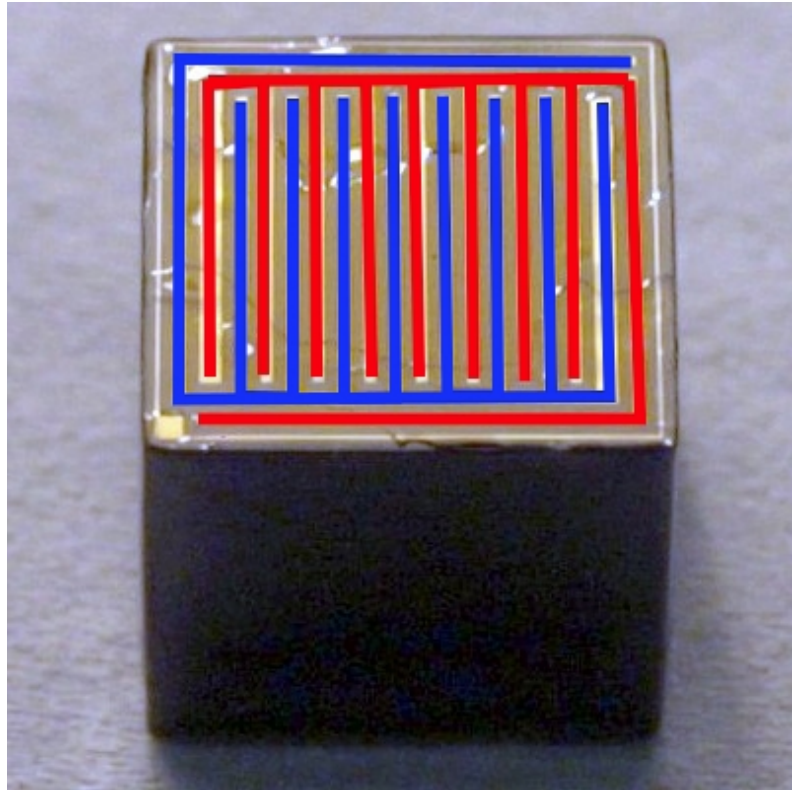


Two comb-shaped, differently biased anode grids create virtual "small pixel effect"

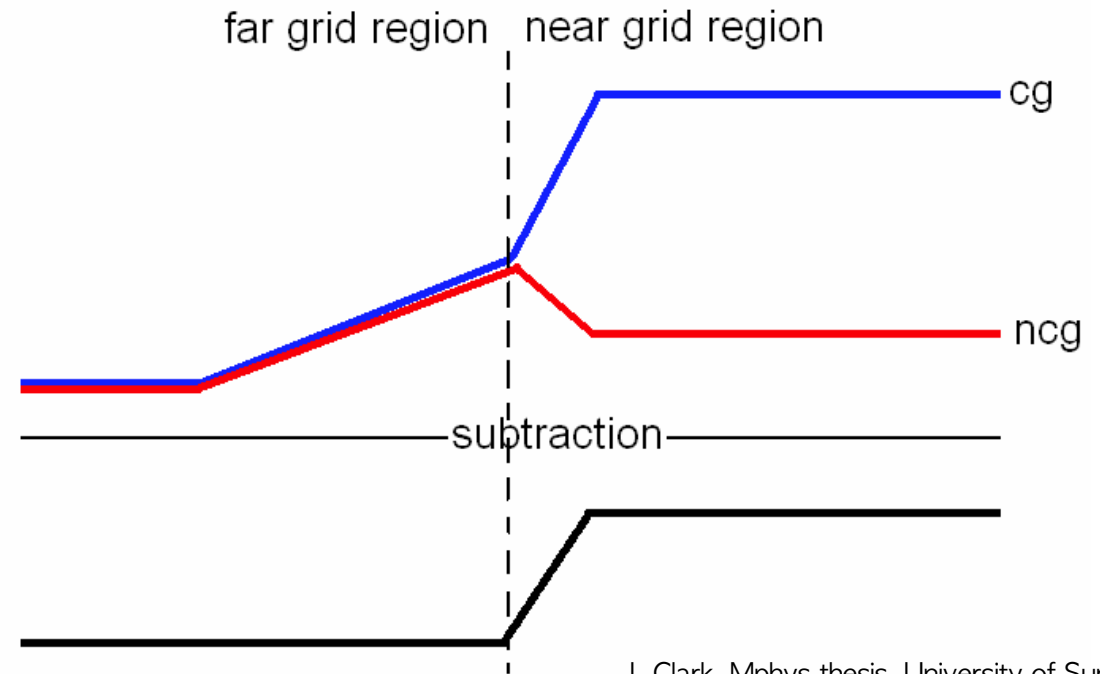


J. Clark, Mphys thesis, University of Surrey

- Fast electron, slow holes
- Electrons reach the near grid region
generation of a signal
- Holes remain in the far grid region
no signal contribution



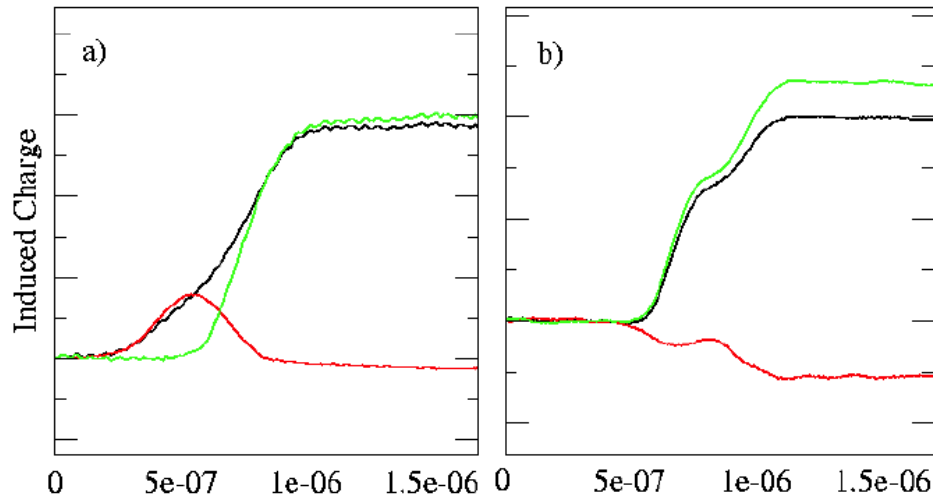
Two comb-shaped, differently biased anode grids create virtual "small pixel effect"



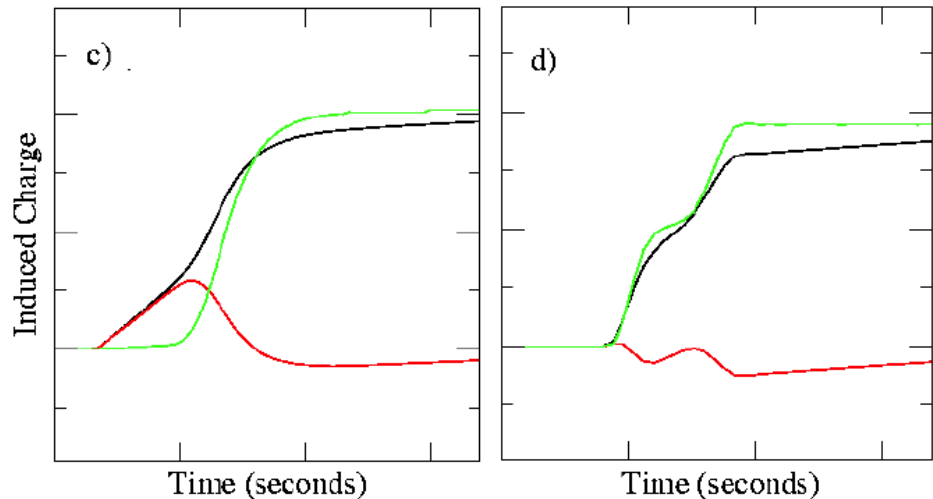
The pulsed signal is the subtraction of the 2 grid signals



Measured



Simulated



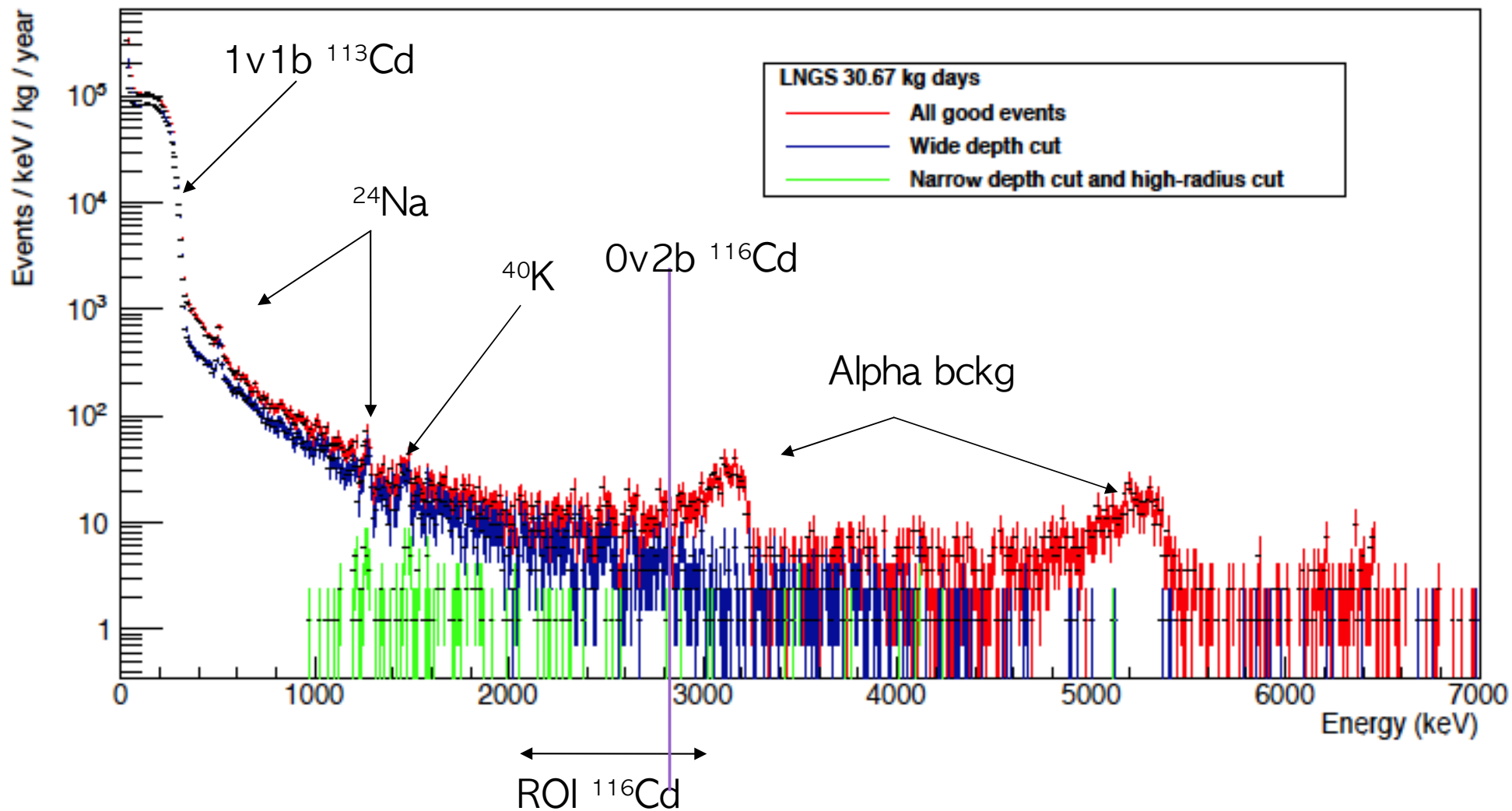
Single-Site Event

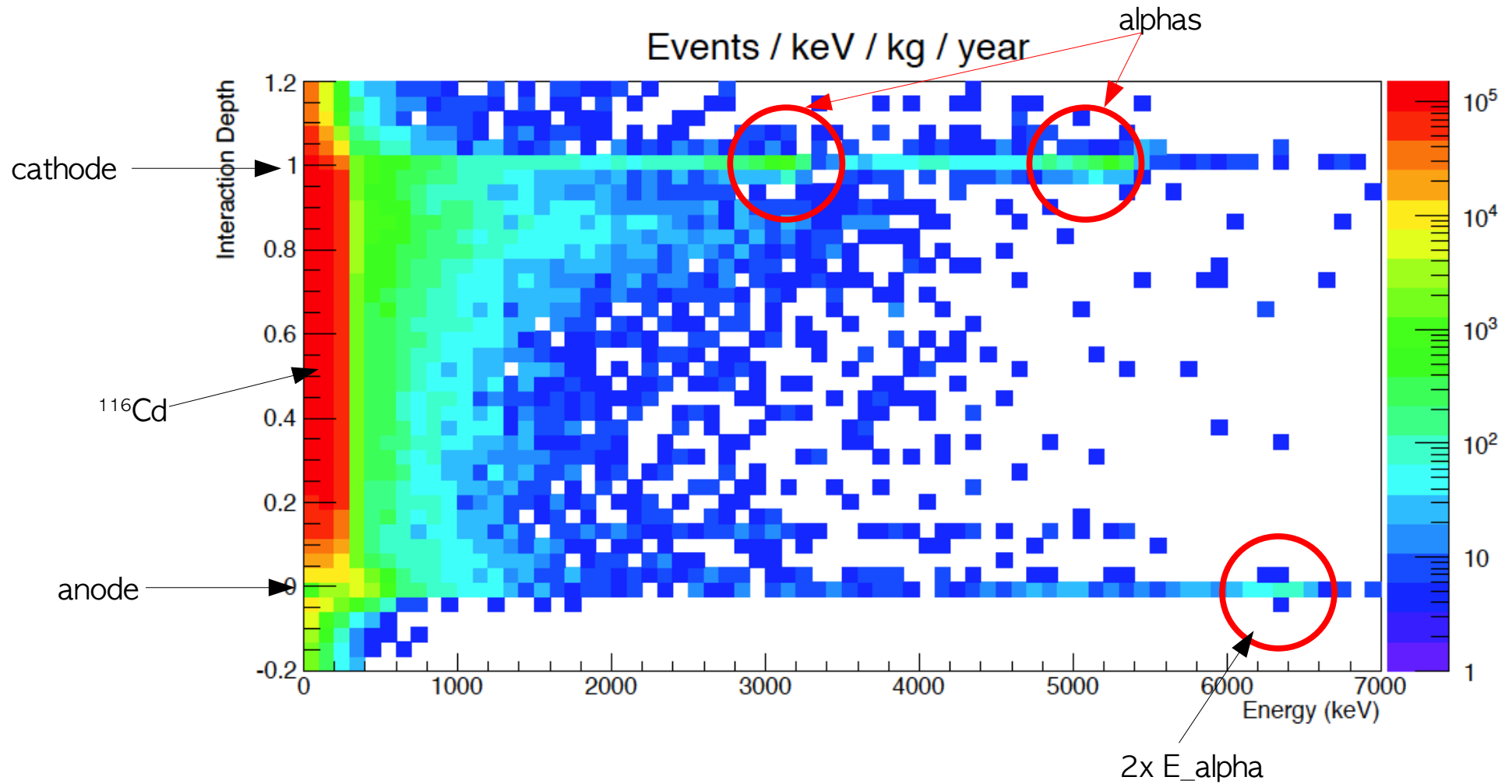
Multi-Site Event

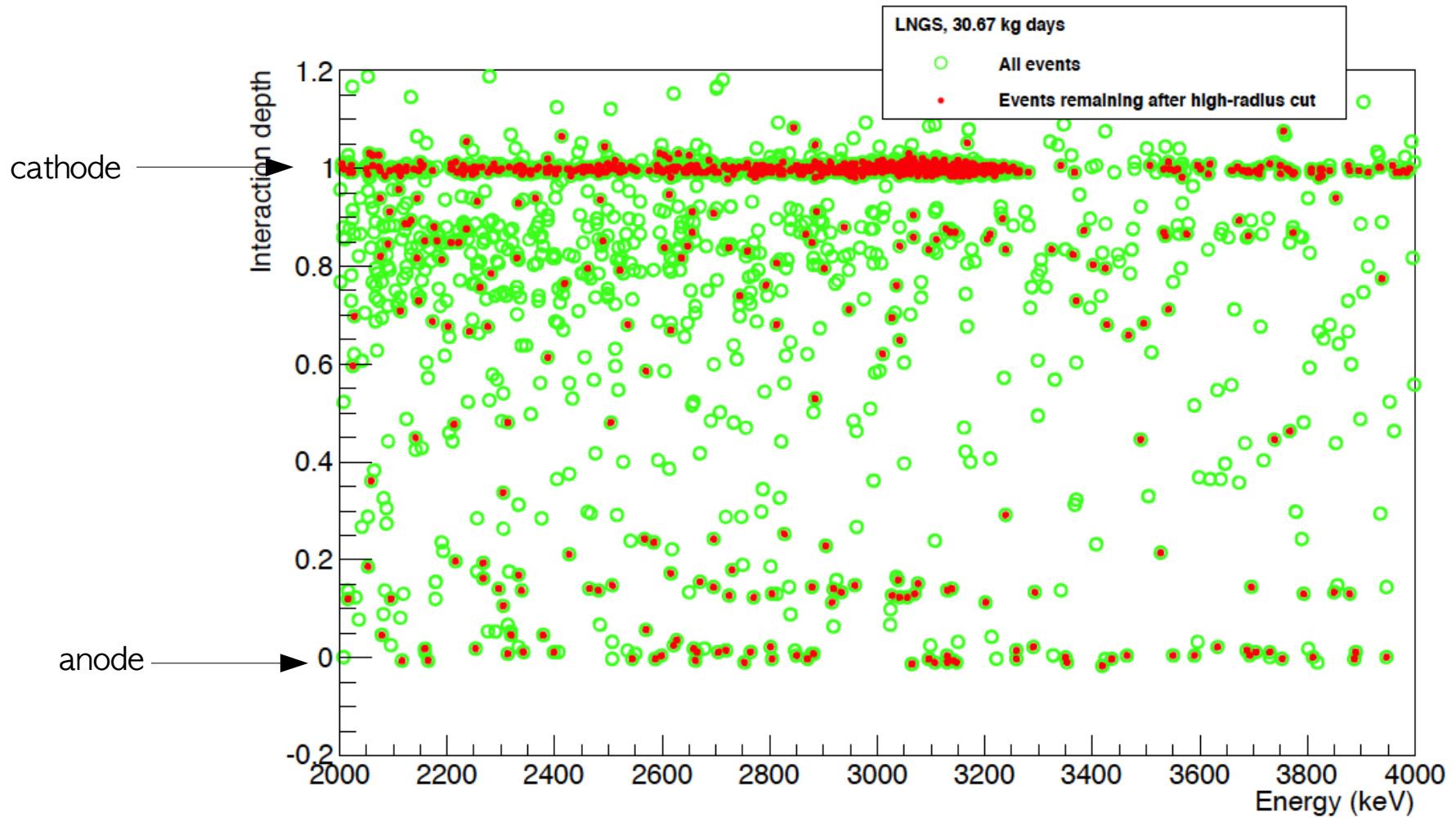
C. Oldorf, TAUP2011

- Pulse Shape with FADC readout:
Distinguish between single site (0v2b)
and multi site events (g-background)
- Depth-sensing allows rejection of
background from surface contamination
Identify noise events

McGrath et al., acc. by NIMA, 2009

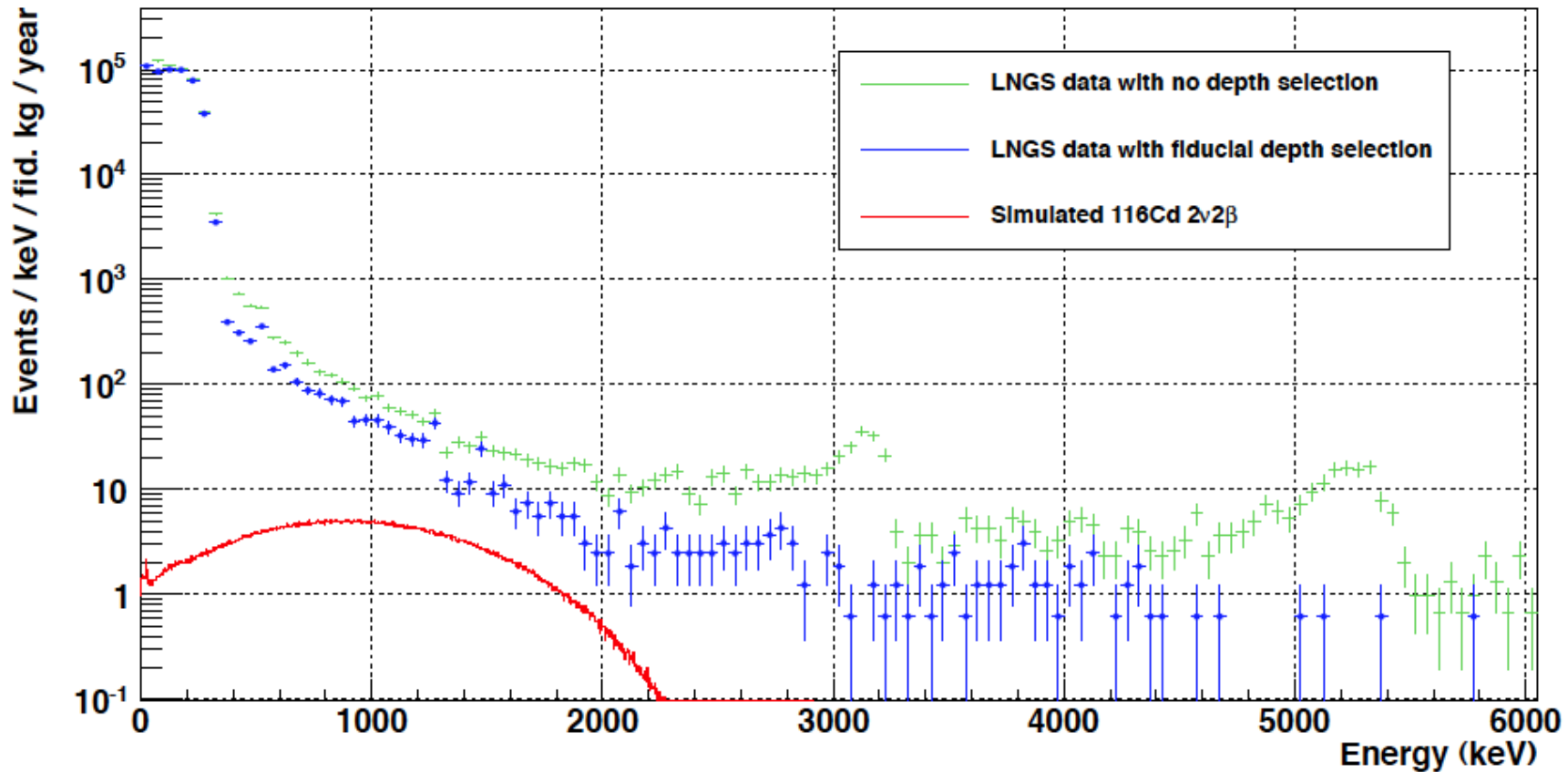








23.6 raw kg days



background rates for our region of interest (2.8 MeV):

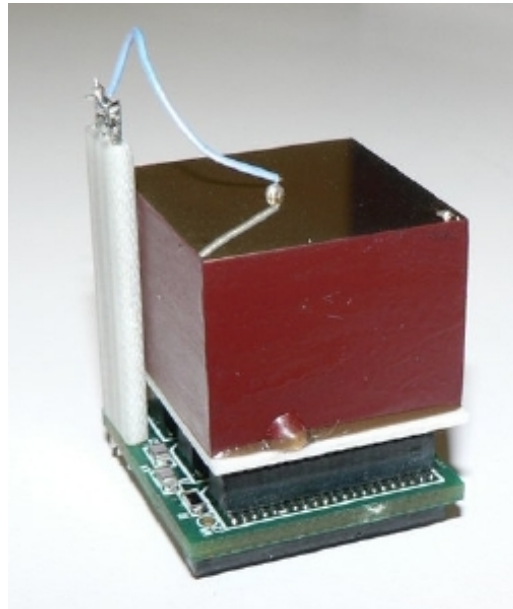
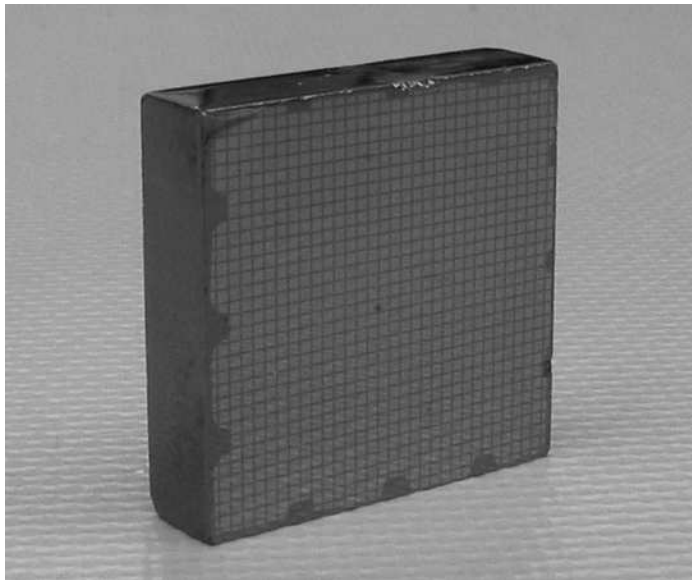
- no depth cut or radius cut: 12 /keV/kg/year
- cathode events removed: 4 /keV/kg/year
- cathode events AND high-radius events removed: 0.6 /keV/kg/year
- optimized (narrower) depth cut and high-radius events removed: 0.13 /keV/kg/year



Pixel detector technology

Two types of detectors under investigation:

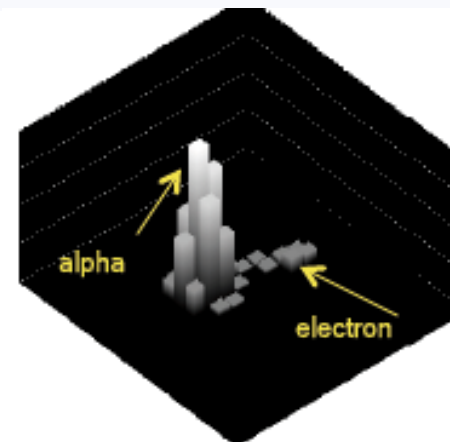
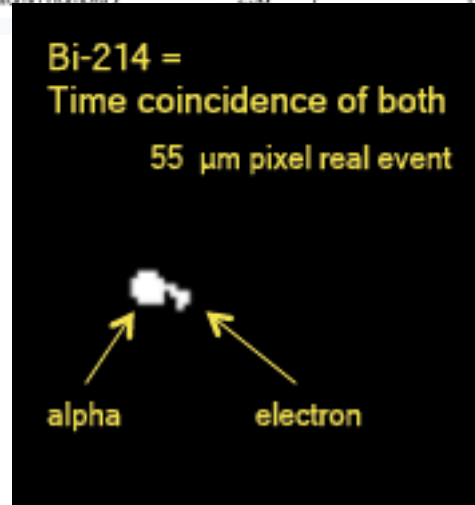
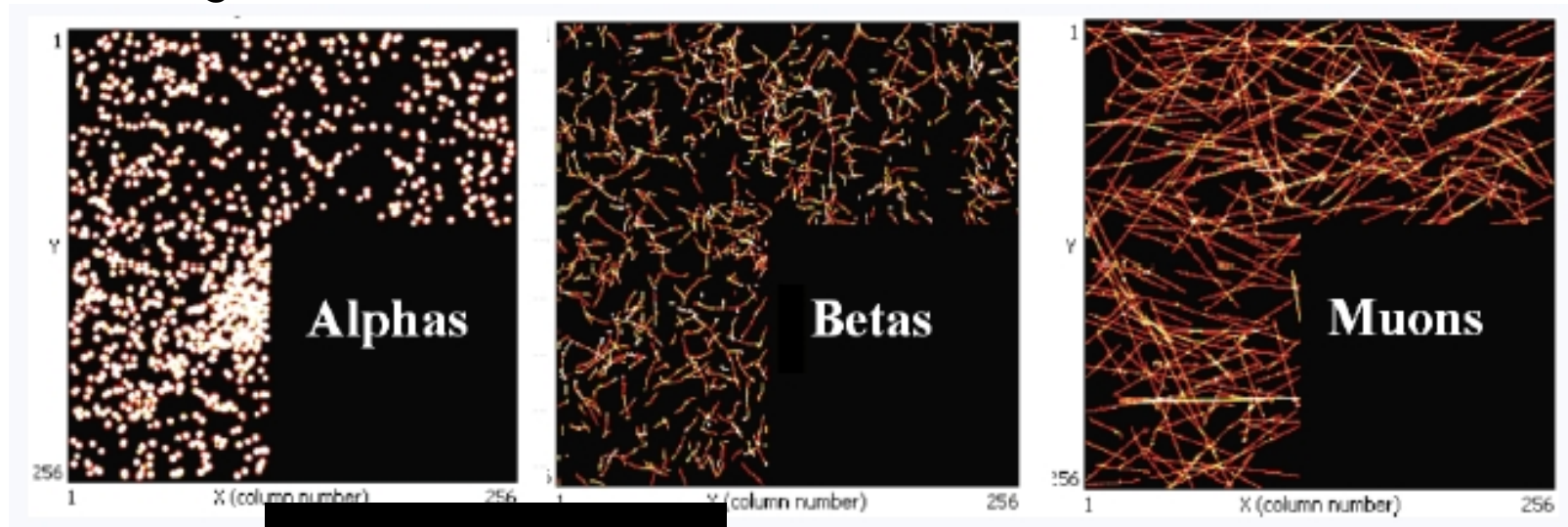
- Large volume ($2 - 6 \text{ cm}^3$) with large pixel pitch ($\sim 1 \text{ mm}$)
Washington University of St. Louis and Polaris System
- Thin detectors ($0.3 - 2 \text{ mm}$) with small pixel pitch ($\sim 100 \mu\text{m}$)
Timepix detector developed by the Medipix2 Collaboration





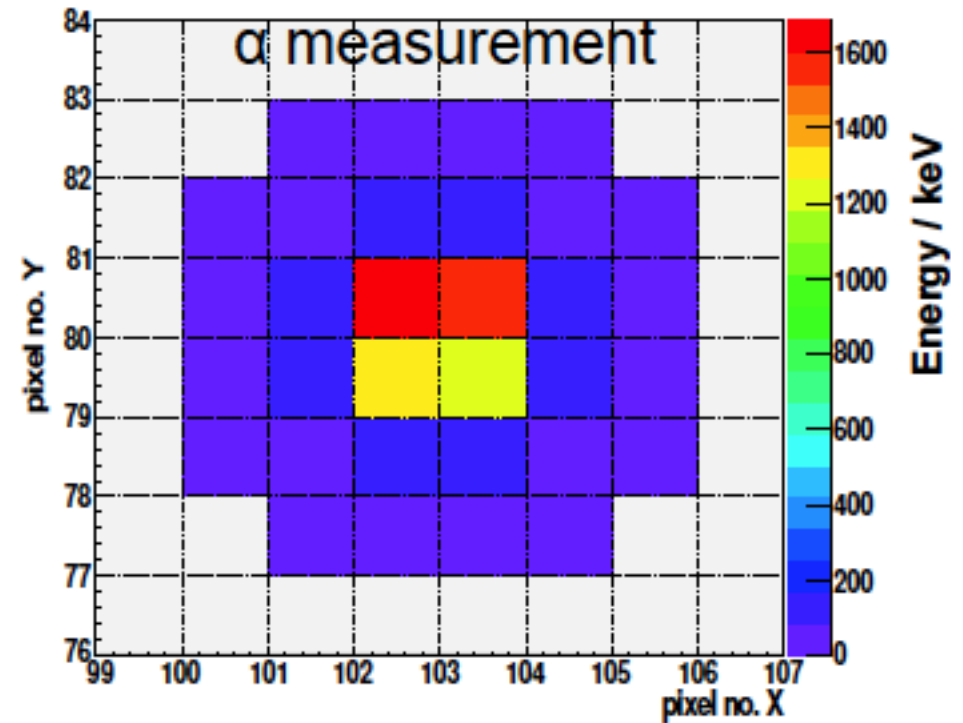
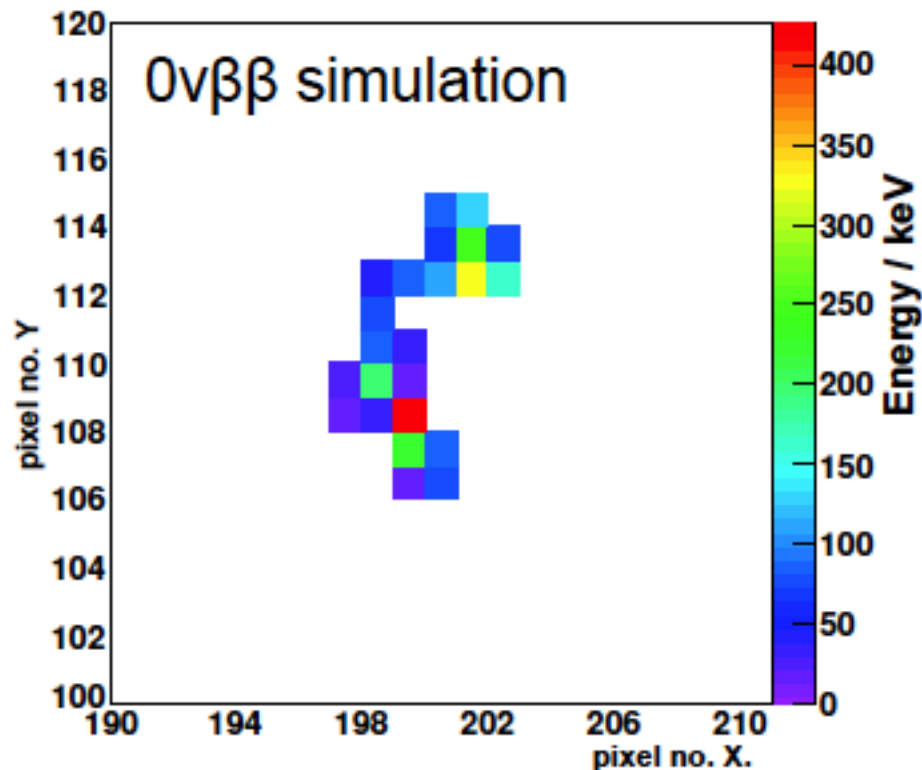
- 2 Si systems: $14 \times 14 \times 0.3\text{mm}^3$
- 2 CdTe systems: $14 \times 14 \times 1\text{mm}^3$
- 256×256 pixel systems
- 128×128 pixel systems

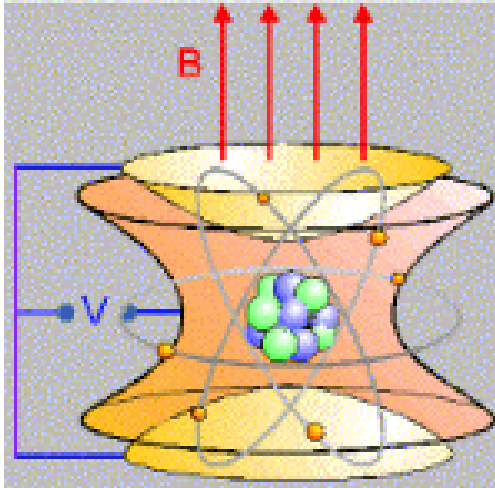
Particle tracking with a solid-state TPC



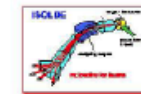


- 2 Si systems: $14 \times 14 \times 0.3 \text{ mm}^3$
 - 2 CdTe systems: $14 \times 14 \times 1 \text{ mm}^3$
 - 256×256 pixel systems
 - 128×128 pixel systems
- Particle tracking with a solid-state TPC





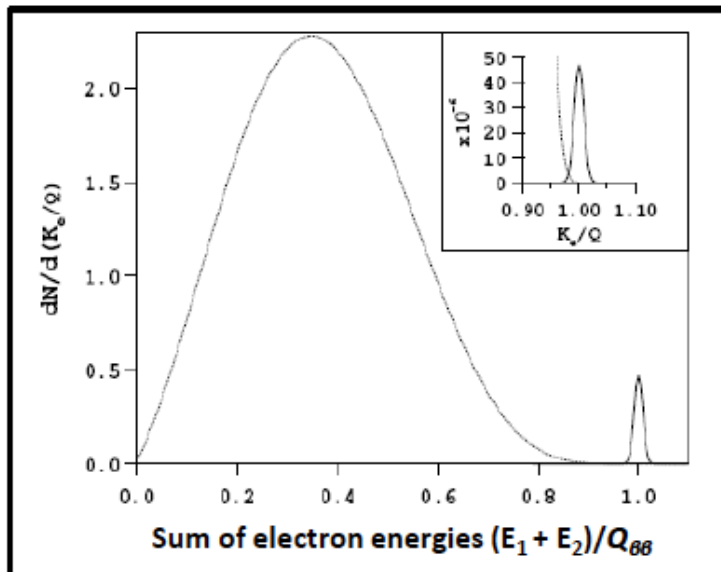
C. Droese, G. Marx, M. Rosenbusch, R. Wolf, L. Schweikhardt, K. Zuber, K. Blaum, C. Böhm, C. Borgmann, R. B. Cakirli, S. Eliseev, D. Fink, S. Kreim, D. Neidherr, D. Beck, M. Block, F. Herfurth, J. Kluge, E. M. Ramirez, G. Audi, D. Lunney, S. Naimi, M. Wang, A. Herlert, M. Kowalska, S. George, S. Schwarz, M. Breitenfeldt



Slides from: J. Stanja, IKTP Seminar, T'U Dresden, 2010
M. Redshaw, ECT, Trento, 3-7 September 2012*

- The mass is a fundamental property which is of interest in different kinds of physics (general physics, nuclear structure physics, etc.)
- Important for determination of Q-values e.g. of neutrinoless double-beta-decay
- There the small amount of signal and the possible vicinity of background lines require precise knowledge of the Q-value
- Few experiments deal with high precision mass measurement using Penning traps like ISOLTRAP at ISOLDE/CERN

$Q_{\beta\beta}$ corresponds to location of $0\nu\beta\beta$ signal



$$Q_{\beta\beta} = [M({}_Z^AX) - M({}_{Z+2}^AY)]c^2$$

$Q_{\beta\beta}$ is required for phase space factor calculation

$$2\nu\beta\beta : G_{2\nu} \sim Q_{\beta\beta}^{11}$$

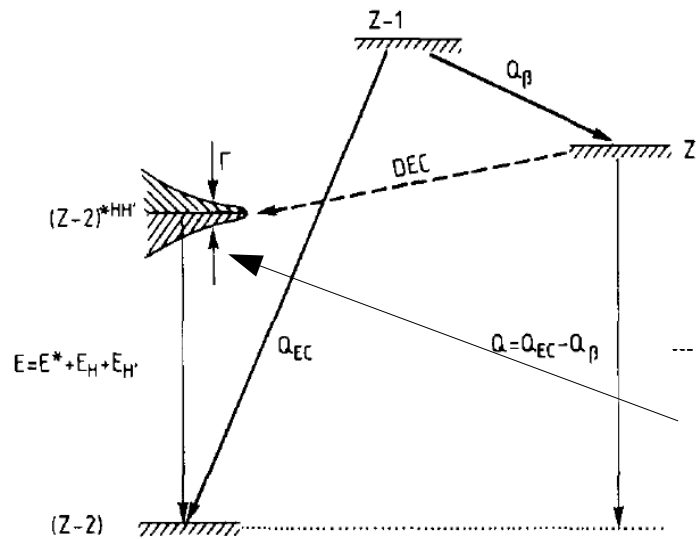
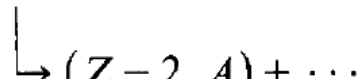
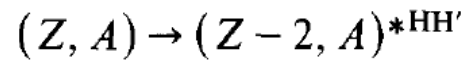
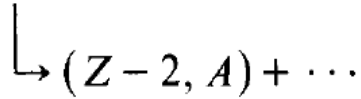
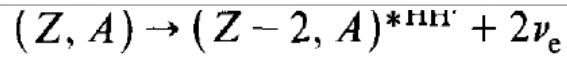
$$\text{For } \frac{\sigma_Q}{Q_{\beta\beta}} = \frac{10 \text{ keV}}{2 \text{ MeV}} \Rightarrow \frac{\sigma_G}{G_{2\nu}} = 5.5 \%$$

$$0\nu\beta\beta : G_{0\nu} \sim Q_{\beta\beta}^5$$

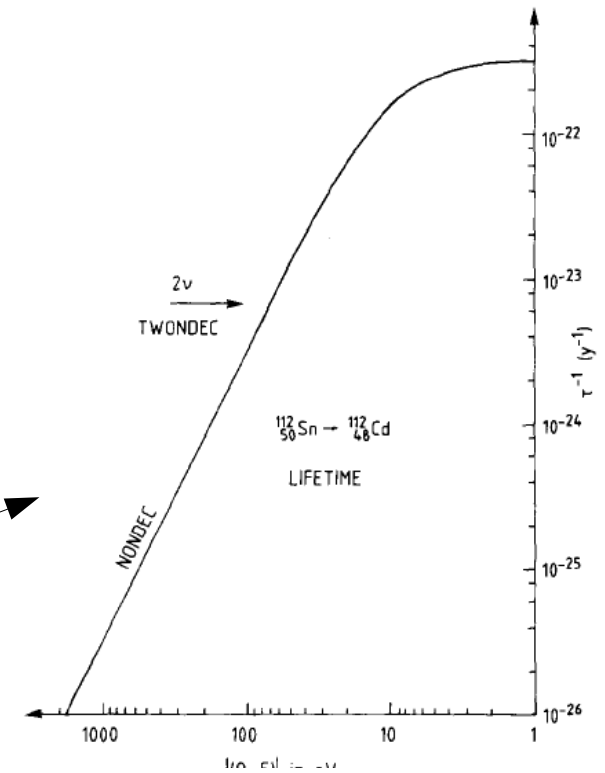
$$\text{For } \frac{\sigma_Q}{Q_{\beta\beta}} = \frac{10 \text{ keV}}{2 \text{ MeV}} \Rightarrow \frac{\sigma_G}{G_{0\nu}} = 2.5 \%$$

Penning Traps: Double EC

Figure from J. Bernabeu, Nuc. Phys. B **223**, 15 (1983)

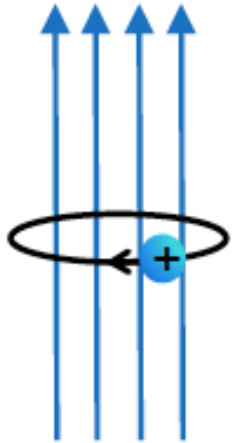


$$\frac{1}{\tau} \approx \frac{(\Delta M)^2}{(Q - E)^2 + \frac{1}{4}\Gamma^2} \Gamma,$$



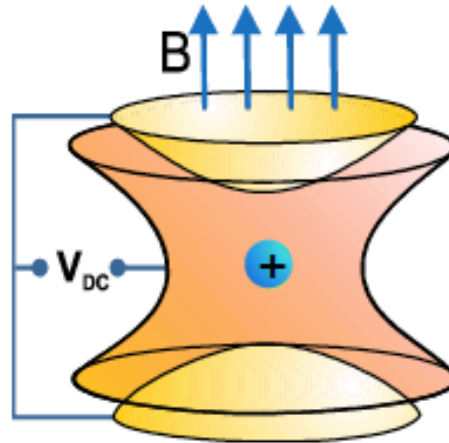
Penning Traps: Working principle

Uniform B-Field



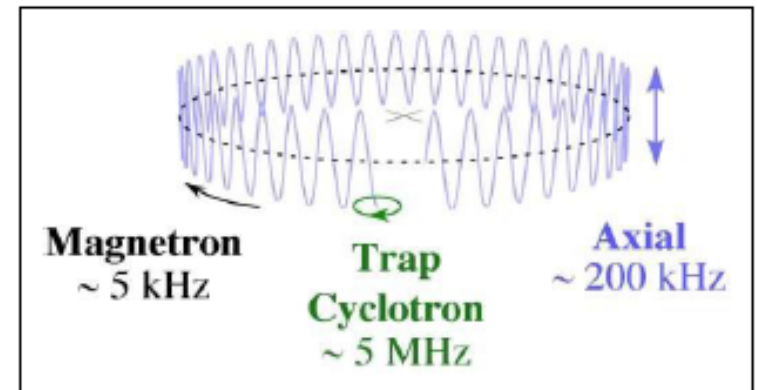
+

Quadrupole E-Field



=

Three Normal Modes



$$\omega_c \approx \omega_{ct} \gg \omega_z \gg \omega_m$$

$$\omega_c = \frac{qB}{m}$$

$\omega_c/2\pi$ = cyclotron frequency
 m = mass
 q = charge
 B = magnetic field strength

$$\omega_c^2 = \omega_{ct}^2 + \omega_z^2 + \omega_m^2$$

$$\omega_c = \omega_+ + \omega_-$$

M. Redshaw, ECT*, Trento

Uniform B-Field



+

Quadrupole E-Field

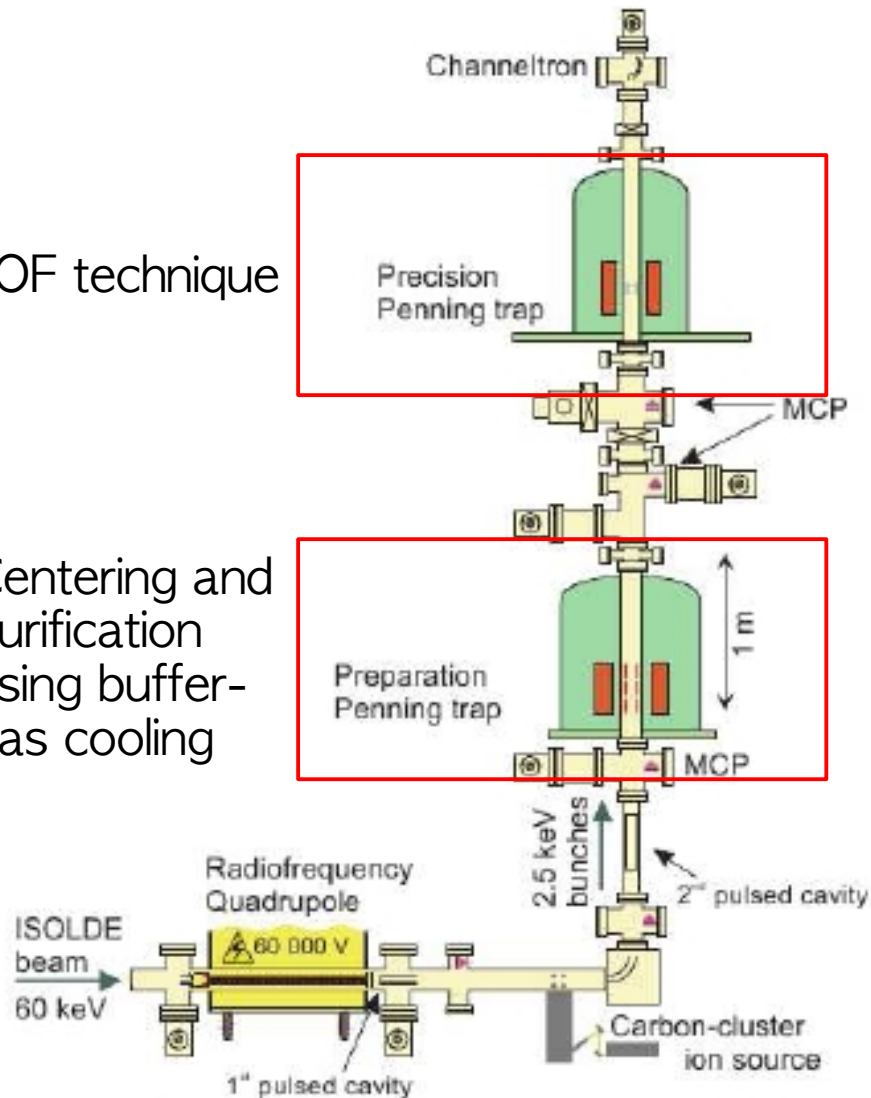


M. Redshaw, ECT*, Trento

Penning Traps: ISOLTRAP

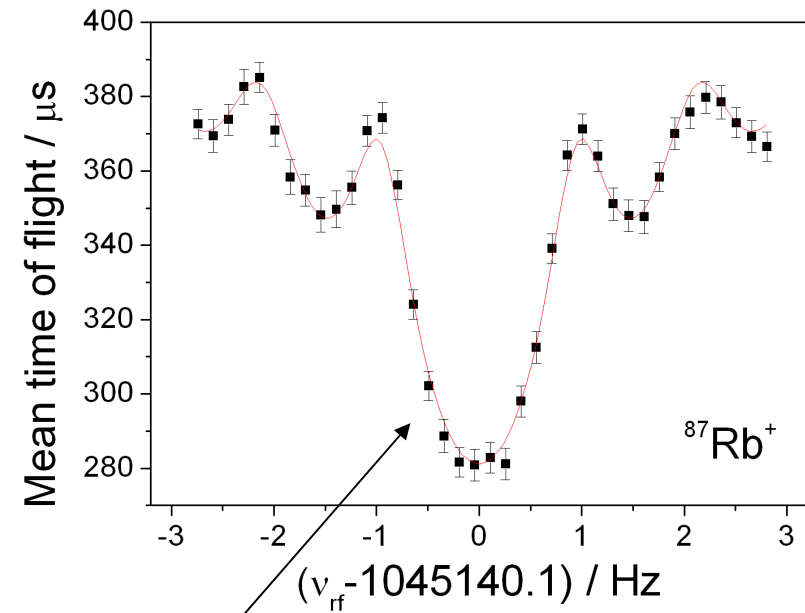
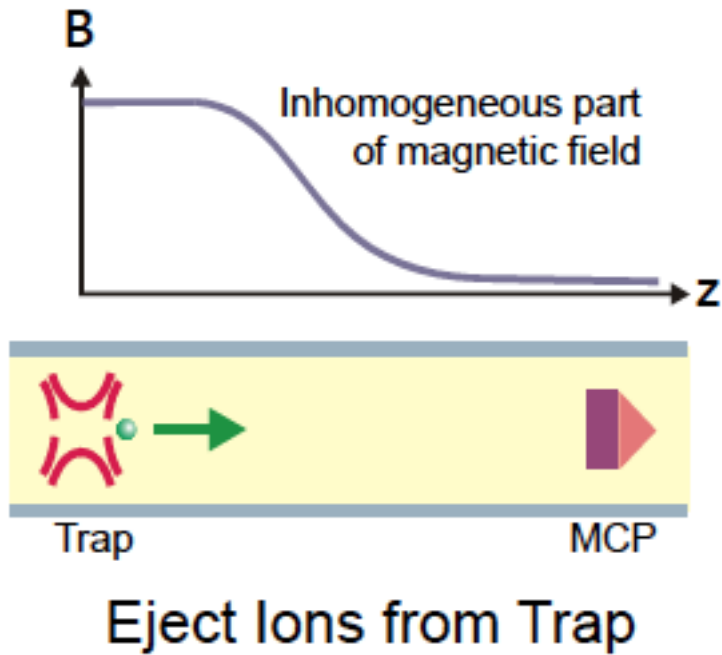
TOF technique

Centering and purification using buffer-gas cooling



- uses up to 60 keV continuous beam of monocharged ions
- reaches a relative uncertainty of $\delta m/m \sim 10^{-8}$
- ions with half-lives of less than 100 ms can be measured
- consists of two Penning traps

J. Stanja, IKTP Seminar



Minimum at cyclotron frequency



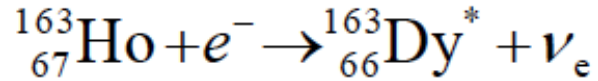
$$Q = m_m - m_d = \left(\frac{\omega_d}{\omega_m} - 1 \right) (m_d - m_e)$$

Isotopes of interest

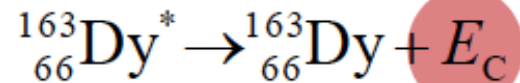
Mother	Daughter	Q-Value (keV)
$^{48}_{20}\text{Ca}$	$^{48}_{22}\text{Ti}$	4274 ± 4
$^{96}_{40}\text{Zr}$	$^{96}_{42}\text{Mo}$	3347.7 ± 2.2
$^{110}_{46}\text{Pd}$	$^{110}_{48}\text{Cd}$	2004 ± 11
$^{116}_{48}\text{Cd}$	$^{116}_{50}\text{Sn}$	2809 ± 4
$^{150}_{60}\text{Nd}$	$^{150}_{62}\text{Sm}$	3367.7 ± 2.2

Data	Ratio r	Q value/keV
30-840-30 ms	1.000 019 713 1(89)	2018.09(90)
50-600-50 ms	1.000 019 708 1(89)	2017.60(90)
Weighted average	1.000 0197 106(63)	2017.85(64)
AME2003		2004(11)

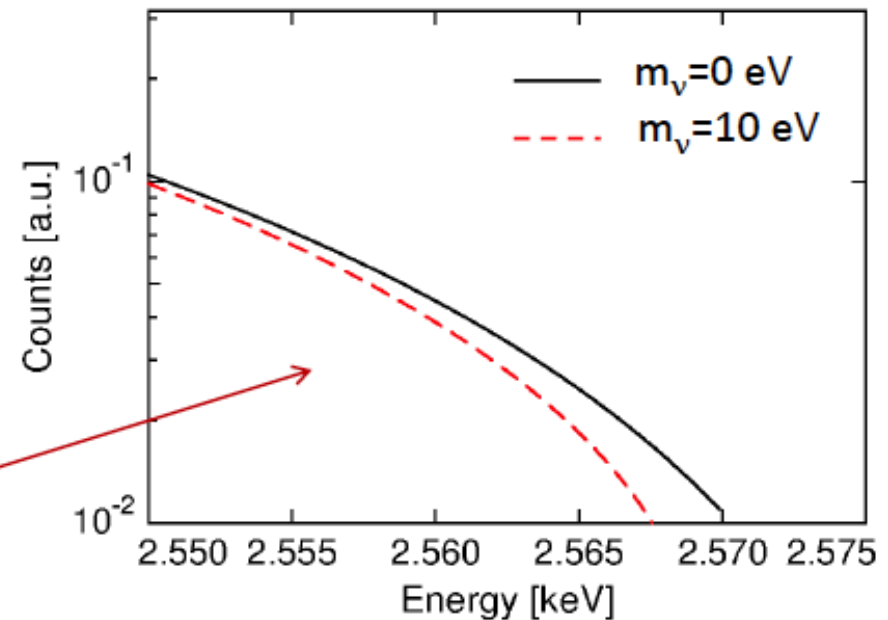
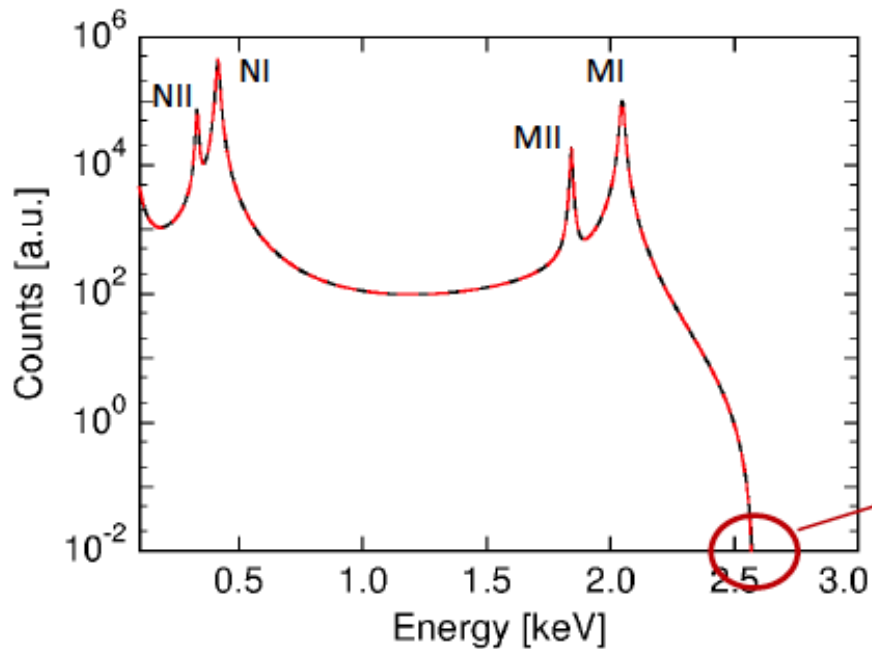
~ 13 keV difference



- $Q_{\text{EC}} \cong 2.5 \text{ keV}$



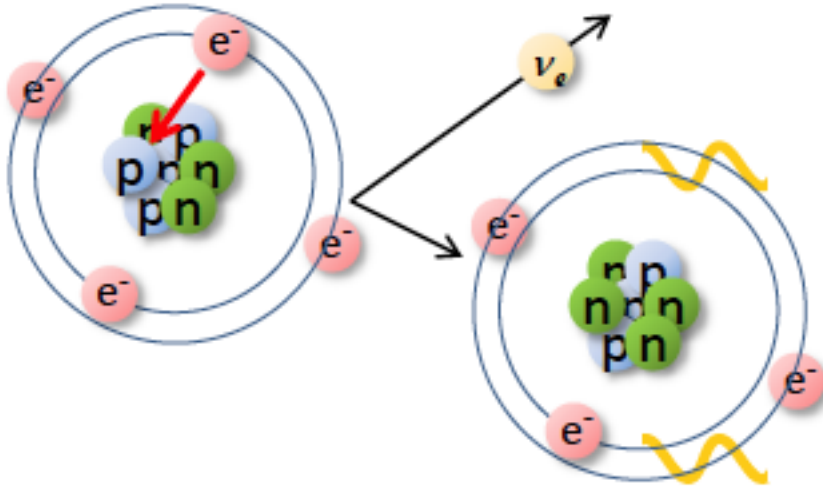
- $\tau_{1/2} \cong 4570 \text{ years}$



Extremely important to measure the end-point **VERY** precisely

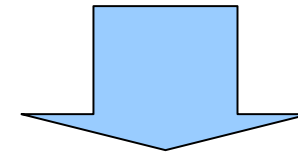
Penning Traps: The case of ^{163}Ho

L. Gastaldo courtesy



The atomic de-excitation is accompanied by:

- X-ray emission
- Auger electrons
- Coster-Kronig transitions



Calorimetric measurement of the energy
SOURCE=DETECTOR

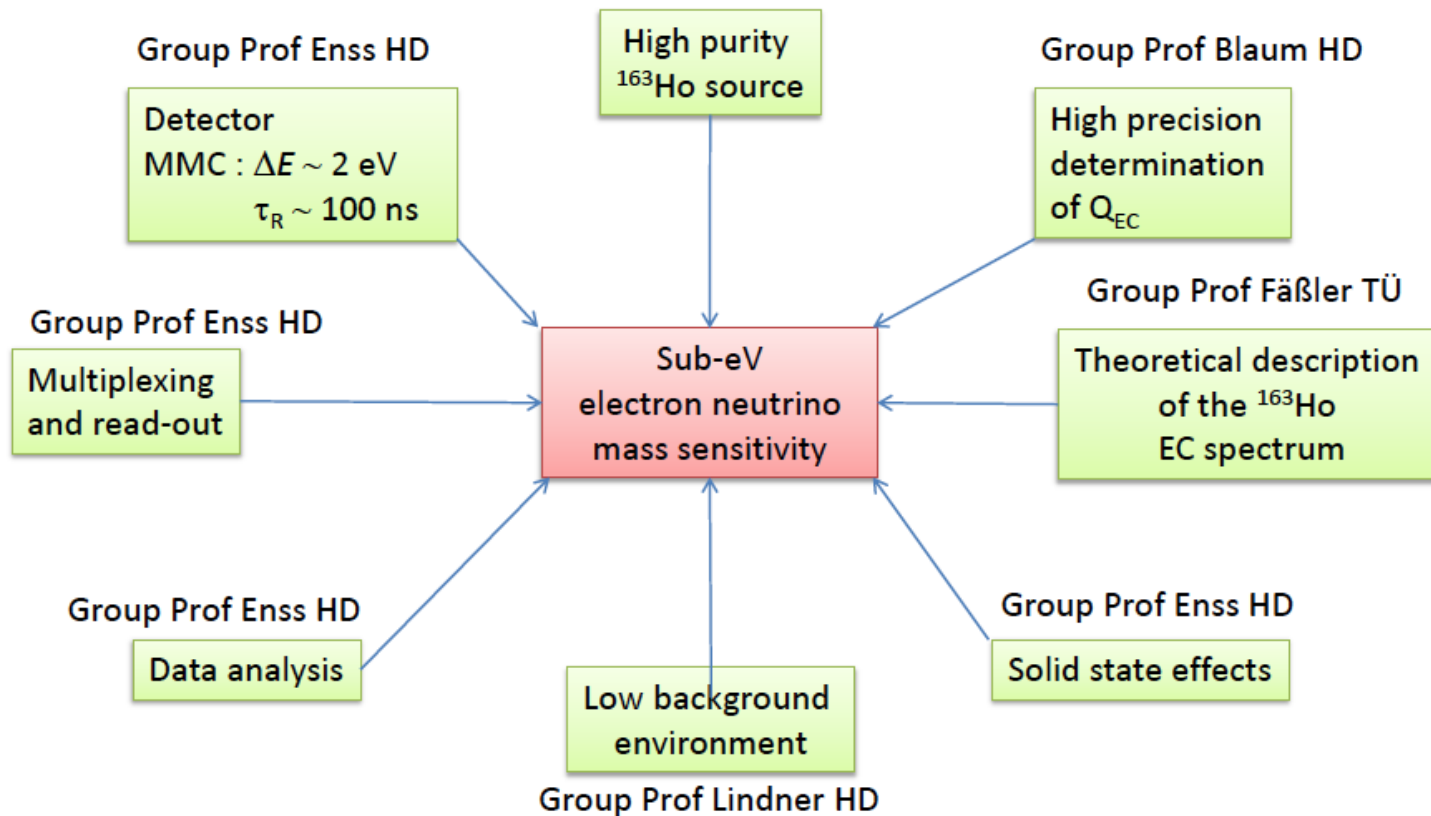
$$\frac{dW}{dE_C} = A(Q_{EC} - E_C)^2 \sqrt{1 - \frac{m_v^2}{(Q_{EC} - E_C)^2}} \sum_H B_H \phi_H^2(0) \frac{\frac{\Gamma_H}{2\pi}}{(E_C - E_H)^2 + \frac{\Gamma_H^2}{4}}$$

The very interesting case:

- very low Q-value (Ho has an end-point energy around 2.5 keV)
- Capture energy very close to Q-value

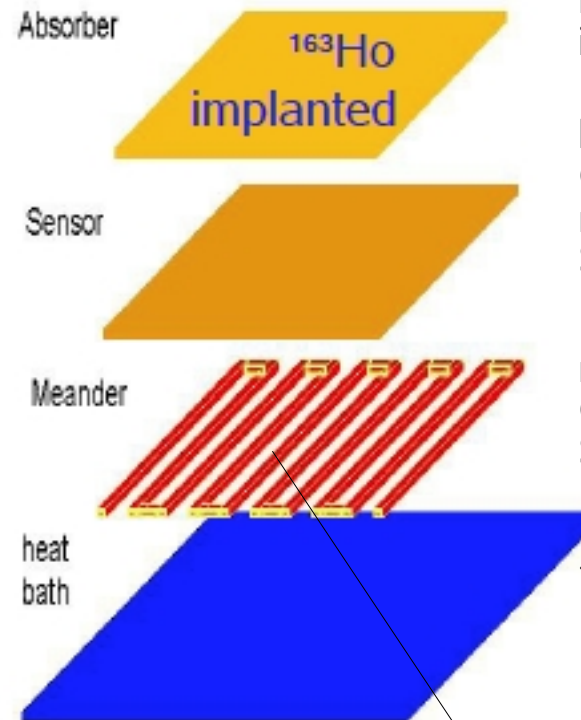
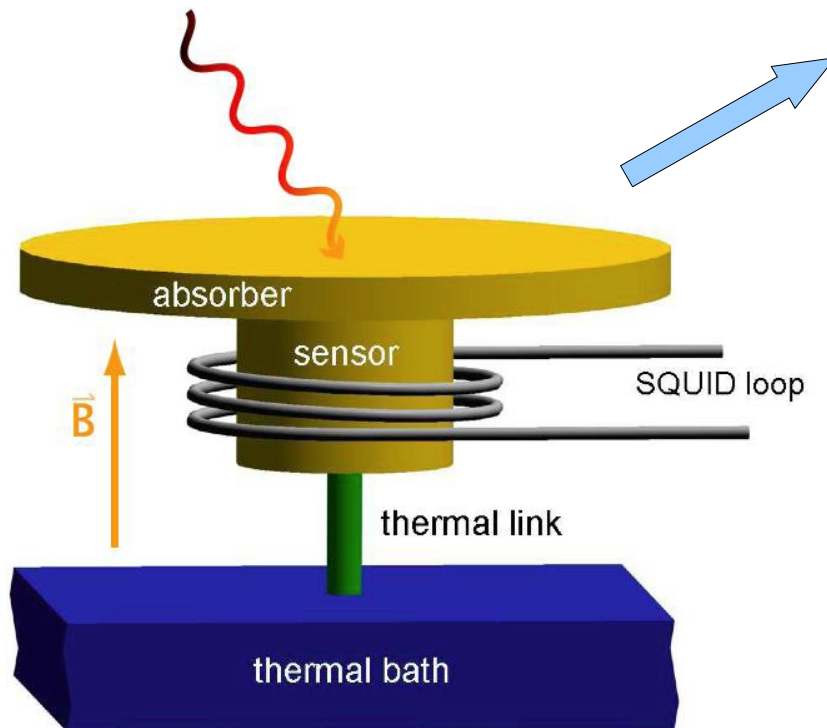
ECHO Experiment

Group Prof Lahiri Kolkata / Prof Szucs
 Group Prof Düllmann MZ/ Dr Eberhardt



Slides from: L. Gastaldo courtesy

Metallic Magnetic Calorimeter



Energy is absorbed in the Au layer \rightarrow temperature increases

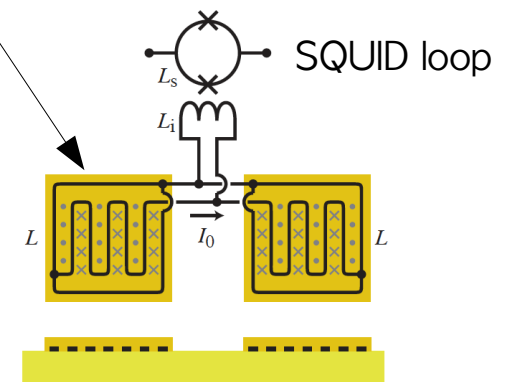
Paramagnetic sensor (Au:Er)
Change in $T \rightarrow$ change in magnetization \rightarrow read out by a SQUID loop

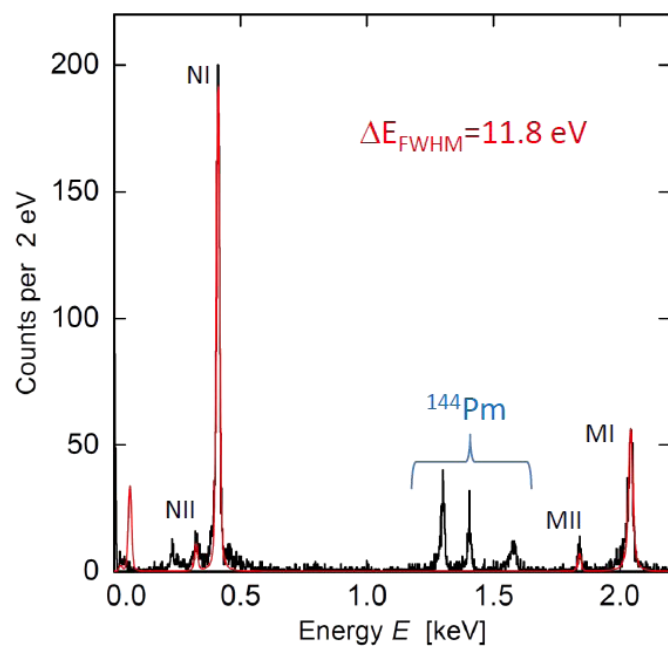
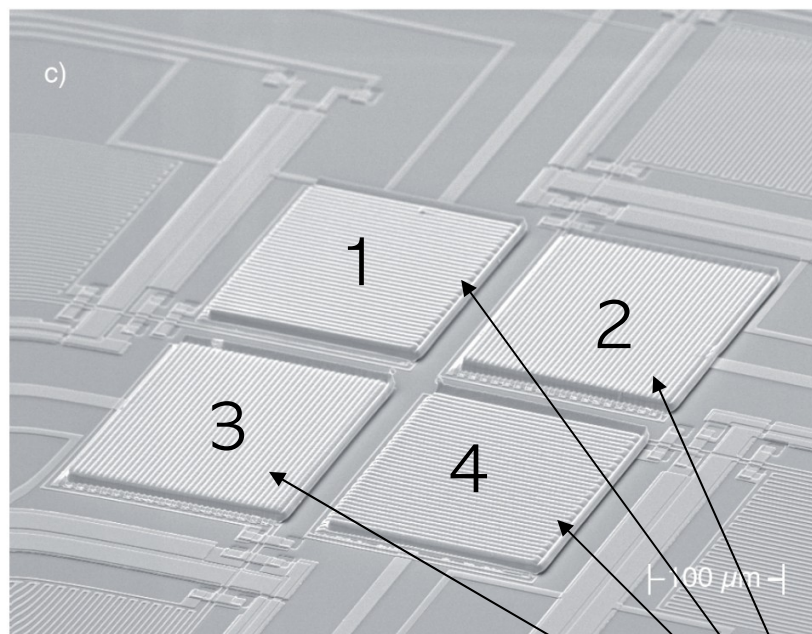
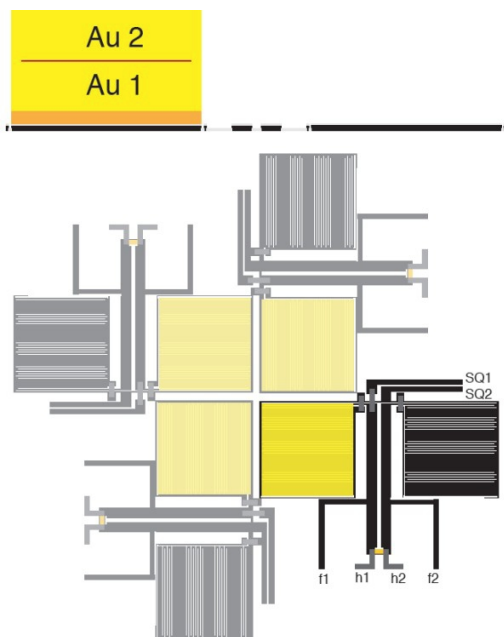
2x Meander pick-up coils to measure magnetic gradient
Connected in parallel to the SQUID loop

$T = \text{few mK}$

Characteristics:

- energy resolution: FWHM 2 eV @ 6keV
- rise time: 90 ns





4 pixels device

Impurities in the flux (beam was not clean)
Main contamination ^{144}Pm

The performance of the detector with and without the Ho layer have been tested:

- Wait 3 months after implantation in order to have short living decaying
- No deviation in temperature behavior
- No deviation in pulse shape and height
- A bit worse energy resolution (from 4.9 eV to 6.6 eV). It can be due to additional noise contribution
- Background events in nearby pixels can be discriminated by different pulse shape and rejected
- Good energy response and linearity
- Problem of background rejection if events are generated in nearby pixels (for instance coming from ^{144}Pm). Cross talks can be eliminated applying a silicone membrane as a detector substrate

the thermal properties of the implanted detector can be understood and are not affected by the implantation process

Plan for a new detector design for crosstalk reduction and better energy resolution from 12eV to 2eV

Required activity in the detectors:

Final experiment $\rightarrow 10^6$ Bq (10^{17}) atoms

Pilot experiment $\rightarrow 10^3$ Bq (10^{14}) atoms (time scale ~ 1 year)

Required Purity: No radioactive contaminants Ratio ^{163}Ho /other ions ~ 1000

Chemical form: depends on the chosen absorber preparation:

ion implantation

dilute alloy

Q- values measurement are very important for the measurement of the neutrino mass/
Majorana neutrino mass.

NME of the $0\nu 2b$ decay strongly depends on the Q-value

The possibility of measuring the neutrino mass from 2EC also strongly depends on the Q-value determination

Calorimetric experiments (ECHO) will provide an independent look at kinematical neutrino mass limits. The scalable approach and further R&D work will allow to reach a competitive level of sensitivity